THE 'KURII' CIRCUIT: A HIGH POWER FACTOR AND LOW COST THREE-PHASE RECTIFIER

Ewaldo L. M. Mehl
Universidade Federal do Paraná
Departamento de Engenharia Elétrica
Caixa Postal 19011
81531-970 Curitiba, Paraná, Brazil
E-Mail: e.mehl@ieee.org

Ivo Barbi
Universidade Federal de Santa Catarina
Departamento de Engenharia Elétrica
Instituto de Eletrônica de Potência - Caixa Postal 5119
88040-970 Florianópolis, Santa Catarina, Brazil
E-Mail: ivo@inep.ufsc.br

Abstract

The 'Kurii' (*) Circuit, a new method to improve the power factor of three-phase rectifiers, is introduced in this paper. The main features of the proposed circuit are low cost, small size, high efficiency and simplicity. The power factor improvement is achieved with three bidirectional active switches rated at a small fraction of the total processed power, and gated at the line frequency. Principle of operation and design procedure, with practical example are also presented. The theoretical analysis was validated with experimental results from a laboratory prototype rated at 7.4 kW and connected to the 220 V, 60 Hz AC system. The same circuit was also used in another prototype rated at 12 kW, with similar results.

Introduction

In the recent past a number of new techniques have been proposed [1]—[3] for improving the power factor of three-phase rectifiers. Among them, the circuit proposed in [4] and shown in Fig. 1a makes use of three low-power four-quadrant switches, each gated on at the line frequency at the instant when the input AC voltage crosses zero. The circuit features low cost, simplicity and high efficiency, and is particularly appropriate for high-power application. However, that converter requires a connection to the neutral wire of the AC system and, due to that connection, a pulsed current is present on the neutral. It was also noticed, in the circuit of Fig. 1a, that the energy stored at the input inductors is responsible for building up high voltage stresses across the switches during the turn-off commutation. Although these voltage stresses can be limited with clamping circuits, the circuit reliability is reduced and losses are increased.

In order to overcome those drawbacks, in this paper an improved rectifier, denominated as the 'Kurii' circuit, is introduced and validated by laboratory prototypes. The new circuit is presented in Fig. 1b and, albeit possessing all the attributes of the one presented in [4], does not require a connection to the neutral wire, operates with lower input current, shows lower harmonic distortion on the input current, and does not need any clamping circuit to prevent excessive overvoltage across the active switches during the turn-off commutation.

Circuit Description and Operation

The voltage sources $\mathbf{V_a}$, $\mathbf{V_b}$ and $\mathbf{V_c}$ in Fig. 1 denote the three-phase AC system and $\mathbf{L_a}$, $\mathbf{L_b}$ and $\mathbf{L_c}$ the input inductors. Diodes $\mathbf{D_1}$ to $\mathbf{D_6}$ are low-frequency rectifiers, and $\mathbf{R_o}$ represents the load. The filter capacitor $\mathbf{C_o}$ in Fig. 1a was replaced by two identical capacitors $\mathbf{C_a}$ and $\mathbf{C_b}$ in Fig. 1b, in order to accomplish a balanced central node between the positive and negative output terminals. On the prototypes, each of the four-quadrant switches $\mathbf{S_a}$, $\mathbf{S_b}$ and $\mathbf{S_c}$ were assembled with a low-power MOSFET connected between the DC nodes of a diode bridge, as in Fig. 1c.

(*) *'Kurii' is the Guarani-Indian word for the fruit of the Araucaria Angustifolia, a native tree from the south region of Brazil. In the past that tree was very abundant, specialy on the states of Paraná and Santa Catarina but, due the intensive exploration in the present century, the Araucaria Angustifolia has become scarse in its native region.*

The resulting circuit is similar to the hysteresis-controlled PWM rectifier presented in [5]; however, in the proposed circuit the switches operate at line frequency and the gating circuit is a very simple one.

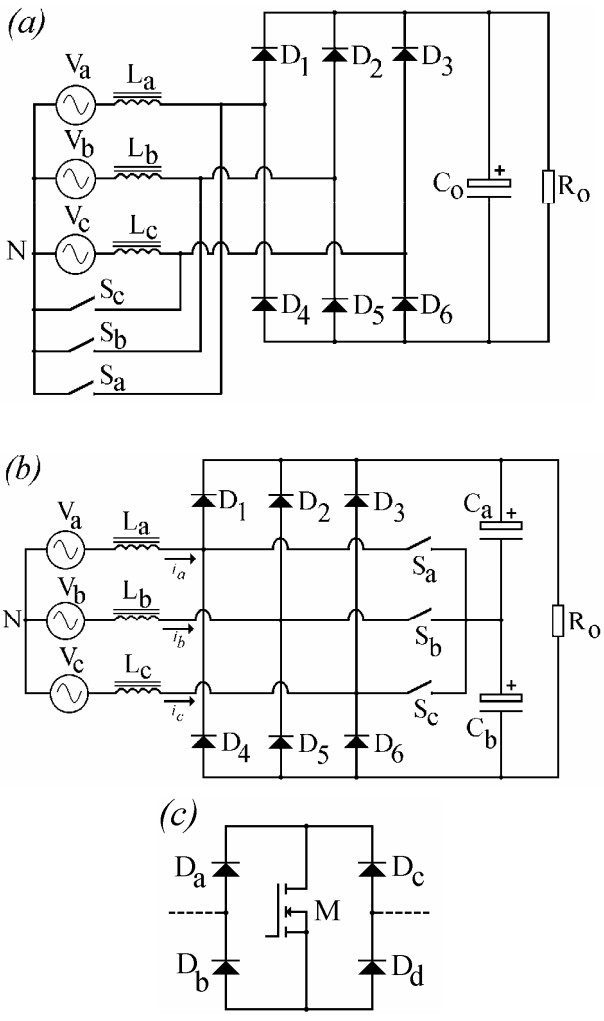

Fig. 1: (a) Circuit presented in [4];
(b) The 'Kurii' Circuit: Improved High Power-Factor Three-Phase Rectifier;
(c) Four-Quadrant Switch used in the prototypes.

Fig. 2 shows the main waveforms of the proposed converter, generated by numerical simulation. On a conventional three-phase diode rectifier, the line current shows a delay of 30° relative to the line voltage, resulting on periodical intervals where such current is null. The effect is a low power factor and high harmonic distortion of the input current. On the proposed

rectifier, the switches $\mathbf{S_a}$, $\mathbf{S_b}$ and $\mathbf{S_c}$ are gated on during an appropriate interval, providing an alternative path for the line current. Each switch is gated on when the corresponding phase voltage is null, with a pulse width denoted by α. On a first approach, α was set to 30° (equivalent to 1.39 ms on a 60 Hz system) for all the load conditions of the converter.

For the circuit analysis, each half-period of the input voltages can be divided in six intervals of 30°, as shown in Fig. 2 for the phase "A". It was also assumed that the inductance L of each input inductor $\mathbf{L_a}$, $\mathbf{L_b}$ and $\mathbf{L_c}$ is such that at the end of the sixth interval ($\theta = 180°$) the current is null. That value will be referred as the *critical inductance* of the rectifier.

On the first interval ($\boldsymbol{t_1}$) the voltage at phase "A" is positive, but the voltage at phase "B" is greater than the voltage at phase "A". As a result, on a conventional three-phase rectifier the current on phase "A" remains null during the first 30° interval. On the proposed circuit, however, the switch $\mathbf{S_a}$ is gated on during that interval. Therefore the input current at phase "A" evolves from zero to a maximum value ruled by (1), where L is the critical inductance, ω is the angular frequency and V is the peak value of the AC phase input voltage:

$$i_a(\theta) = \frac{V}{\omega \cdot L}(1 - \cos\theta) \tag{1}$$

From (1), for $\theta = 30°$ the value of the current i_a is:

$$i_a(30°) = \frac{V}{\omega \cdot L}\left(1 - \frac{\sqrt{3}}{2}\right) \tag{2}$$

The diodes $\mathbf{D_2}$ and $\mathbf{D_6}$ are on during $\boldsymbol{t_1}$. Therefore the current i_a is divided by two at the central node between the capacitors $\mathbf{C_a}$ and $\mathbf{C_b}$, and returns to the three-phase system through $\mathbf{D_2}$ (*subtracted* from the load current) and through $\mathbf{D_6}$ (*added* to the load current).

At $\theta = 30°$ the switch $\mathbf{S_a}$ can be gated off, because the diode $\mathbf{D_1}$ starts conduction. As a result, on the interval from 30° to 60° ($\boldsymbol{t_2}$) the three switches are off, so the converter behaves like a conventional rectifier with input inductors. The input current evolves ruled by (3), and expression (4) shows the value for $\theta = 60°$:

$$i_a(\theta) = \frac{V}{\omega \cdot L}\left(\frac{9}{7} - \cos\theta - \frac{12 \cdot \theta}{7 \cdot \pi}\right) \tag{3}$$

$$i_a(60°) = \frac{V}{\omega \cdot L}\left(\frac{3}{14}\right) \tag{4}$$

During $\boldsymbol{t_3}$, on a conventional three-phase rectifier the current on phase "B" would be null. Consequently on the proposed rectifier the switch $\mathbf{S_b}$ is gated on from $\theta = 60°$ until $\theta = 90°$. As the voltage on phase "B" is negative, the current pulse through $\mathbf{S_b}$ is opposite to the one presented in $\mathbf{S_a}$ during $\boldsymbol{t_1}$, but is ruled on the same way by (1). As the diodes $\mathbf{D_1}$ and $\mathbf{D_6}$ are on, now that current pulse is divided by two and *added* to the load current at phase "A" and *subtracted* from the load current at phase "C". The input current at phase "A" is ruled by (5), and at $\theta = 90°$ the value of that current is given by (6):

$$i_a(\theta) = \frac{V}{\omega \cdot L}\left(\frac{11}{7} - \cos\theta - \frac{18 \cdot \theta}{7 \cdot \pi}\right) \tag{5}$$

$$i_a(90°) = \frac{V}{\omega \cdot L}\left(\frac{2}{7}\right) \tag{6}$$

Over the period $\boldsymbol{t_4}$, from $\theta = 90°$ to $\theta = 120°$, the three switches are off and again the converter performs like the conventional three-phase rectifier. The diodes $\mathbf{D_1}$, $\mathbf{D_5}$ and $\mathbf{D_6}$ are on, and the input current is given by (7):

$$i_a(\theta) = \frac{V}{\omega \cdot L}\left(2 - \cos\theta - \frac{24 \cdot \theta}{7 \cdot \pi}\right) \tag{7}$$

At $\theta = 120°$, the input current reaches the same value of $\theta = 60°$:

$$i_a(120°) = \frac{V}{\omega \cdot L}\left(\frac{3}{14}\right) \tag{8}$$

During $\boldsymbol{t_5}$ the switch $\mathbf{S_c}$ is gated on. The diodes $\mathbf{D_1}$ and $\mathbf{D_5}$ are on. Due to the voltages' polarities at that interval, the current pulse $\boldsymbol{i_c}$ appears at phase "A" divided by two and is *subtracted* from the load current, and at phase "B" is divided by two and *added* to the load current. The input current at phase "A" is given by (9), and at $\theta = 150°$ the current has the value given by (10):

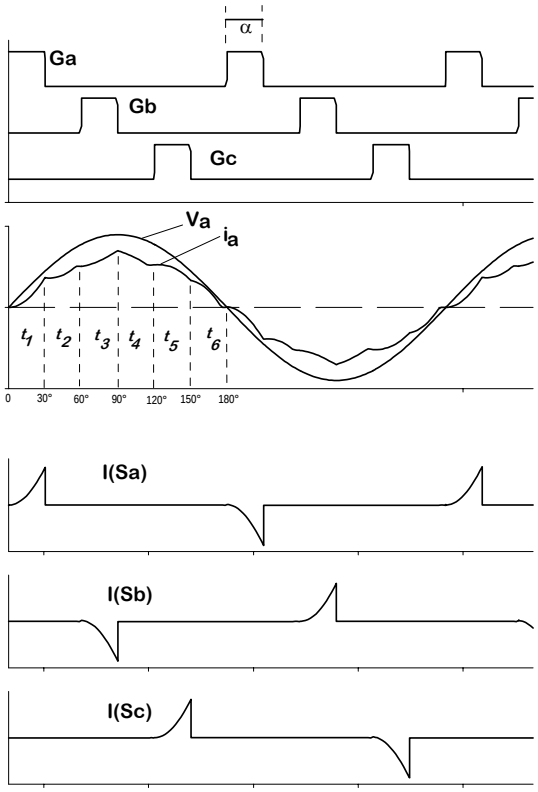

Fig. 2: Main waveforms of the proposed converter.
From top to down, it is shown:
- the 30° gate pulses (G_a, G_b and G_c) for the three active switches S_a, S_b and S_c;
- the phase voltage V_a and the input current i_a;
- the current pulses on the actives switches S_a, S_b and S_c;

$$i_a(\theta) = \frac{V}{\omega \cdot L}\left(\frac{10}{7} - \cos\theta - \frac{18 \cdot \theta}{7 \cdot \pi}\right) \tag{9}$$

$$i_a(150°) = \frac{V}{\omega \cdot L}\left(\frac{\sqrt{3}}{2} - \frac{5}{7}\right) \tag{10}$$

Finally, on $\boldsymbol{t_6}$ (from $\theta = 150°$ to $\theta = 180°$) the circuit behaves again as a conventional three-phase rectifier, since the three switches are off. The diodes $\mathbf{D_1}$, $\mathbf{D_3}$ and $\mathbf{D_5}$ are on. The input current on phase "A" is ruled by (11) in that interval:

$$i_a(\theta) = \frac{V}{\omega \cdot L}\left(\frac{5}{7} - \cos\theta - \frac{12 \cdot \theta}{7 \cdot \pi}\right) \quad (11)$$

As a result of the using of the critical inductance, at $\theta = 180°$ the current is null:

$$i_a(180°) = 0 \quad (12)$$

From $\theta = 180°$ to $\theta = 360°$ the same expressions (1)....(12) can be used, with opposite signs. The analysis can also be extended to the other phases with the appropriate 120° and 240° displacement.

The value of the critical inductance can be calculated with (13), where *P* is the DC power output of the rectifier:

$$L = \frac{54 \cdot V^2}{7 \cdot \omega \cdot \pi^2 \cdot P}\left(2\sqrt{3} - 3\right) \quad (13)$$

Using the appropriate critical inductance with $\alpha = 30°$ and nominal load condition, the output DC voltage ($\boldsymbol{V_o}$) of the circuit is given by (14):

$$V_o = \frac{36}{7 \cdot \pi} V \quad (14)$$

The laboratory prototypes demonstrate that the proposed technique conducts to a dramatic reduction on the harmonic distortion of the input current and an increase of the power factor, contrasting with the traditional three-phase diode rectifier. It was also detected with the prototypes that for a fixed load, a small reduction in α leads to a decrease on the output voltage. As a consequence, if α is set to 30° for the nominal load condition of the rectifier, the conduction angle α can be adopted as the control variable to perform the output voltage regulation and complying a high power factor over a significant range of the output power.

Design Example and Simulation

In order to illustrate the critical inductance and the switches' current calculation, it is assumed a converter with the following specifications:

- AC line input voltage: V_i = 220 V
- AC frequency: f = 60 Hz
- Output power: P = 7.4 kW

The critical inductance is obtained from (15), adapted from (13):

$$L = \frac{54 \cdot V_i^2}{14 \cdot f \cdot \pi^3 \cdot P}\left(\frac{2}{3}\right)\left(2\sqrt{3} - 3\right) \quad (15)$$

With the present values, (15) gives L = 4.19 mH.

Using the critical inductance, the output DC voltage for nominal load can be calculated with (16), adjusted from expression (14):

$$V_o = \frac{36}{7 \cdot \pi} V_i \frac{\sqrt{2}}{\sqrt{3}} = \frac{36}{7 \cdot \pi}(220)\frac{\sqrt{2}}{\sqrt{3}} = 294.1 \text{ V} \quad (16)$$

In practice, the input inductance can be adopted at a slightly lower value than the critical one calculated with (15). As a consequence, the rounded value was chosen:

$$\mathbf{L_a} = \mathbf{L_b} = \mathbf{L_c} = 4 \text{ mH}$$

As seen formerly, the current pulses presented at the switches $\mathbf{S_a}$, $\mathbf{S_b}$ and $\mathbf{S_c}$ are ruled by (1). For α=30°, the peak current ($\boldsymbol{I_{S(pk)}}$) on the switches is given by (17):

$$I_{S(pk)} = \frac{\sqrt{2} \cdot V_i}{2 \cdot \pi \cdot f \cdot L \cdot \sqrt{3}}\left[1 - \frac{\sqrt{3}}{2}\right] \quad (17)$$

With the present values, (17) gives the peak value of 15.96 A. The *rms* value of that current can be calculated with (18):

$$I_{S(rms)} = \sqrt{\frac{1}{\pi}\int_0^{30°}\left\{\left(\frac{\sqrt{2} \cdot V_i}{2 \cdot \pi \cdot f \cdot L \cdot \sqrt{3}}\right)(1 - \cos\alpha)\right\}^2 d\alpha} \quad (18)$$

From (18), a $I_{S(rms)}$ value of 2.93 A is obtained.

Fig. 3 shows the phase input voltage and current of the rectifier, and the current through one of the switches, accomplished by circuit simulation with:

Input voltage sources: $\mathbf{V_a} = \mathbf{V_b} = \mathbf{V_c}$ = 127 V (*rms*)

Input inductors: $\mathbf{L_a} = \mathbf{L_b} = \mathbf{L_c}$ = 4 mH

Output capacitors: $\mathbf{C_a} = \mathbf{C_b}$ = 600 μF

Load resistance: $\mathbf{R_o}$ = 11.6 Ω

Conduction angle of the switches: α = 30°

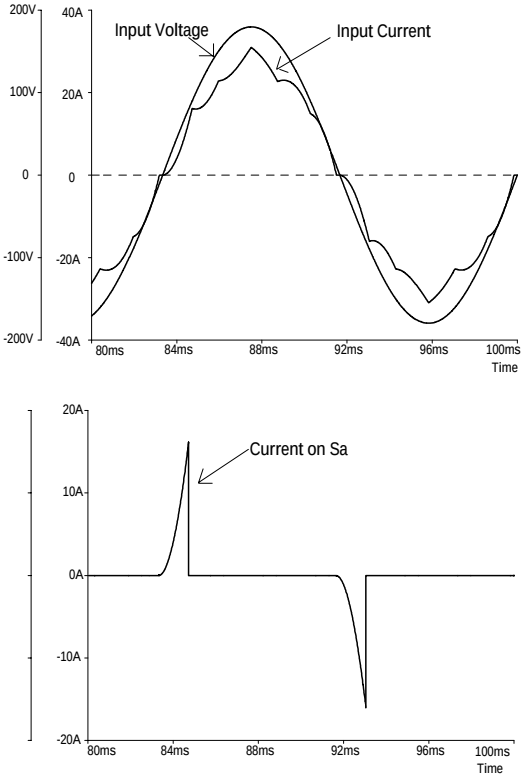

Fig. 3: Simulation results: Input Voltage and Current for 7.4 kW power output, and current through switch S_a, for α = 30°.

Each of the three switches $\mathbf{S_a}$, $\mathbf{S_b}$ and $\mathbf{S_c}$ was simulated using a voltage-controlled switch, with three pulsed voltage sources to produce the appropriate gating signals. Therefore, when the control voltage was set to the "high" value, the corresponding switch was simulated as a 0.1 Ω resistor. When the control voltage was zero, the switch was replaced by a 1 MΩ resistor. With a 11.6 Ω load resistance, the average output voltage obtained was 293.8 V, that leads to an average output power of 7.44 kW. The current pulses through one of the switches are also shown in Fig. 3, for $\alpha = 30°$. The measured peak value is 16.1 A, which agrees with the previously calculated value of 15.96 A.

The Fourier analysis of the current waveform shown in Fig. 3 is presented in Fig. 4. The dominant harmonic component is the 7th, with 4.13%. The 3rd harmonic component is not present, since there is no connection to the neutral wire. The Total Harmonic Distortion (THD) is 4.96 % and the resulting power factor is 0.997.

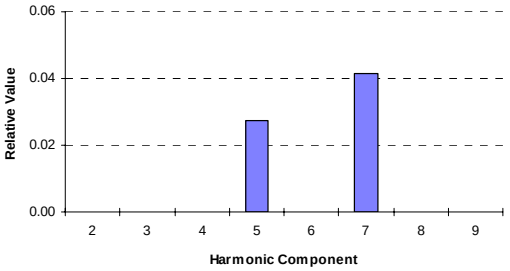

Fig. 4: Relative values of the nine first harmonic components of the simulated input current. The 60 Hz component (not shown) was set to the unity.

Experimental Results

The first laboratory prototype assembled to validate the proposed technique has its main characteristics as follows, and circuit diagram as in Fig. 1b:

- Input line voltage: V_i = 220 V, 60 Hz.
- Rated output DC voltage: V_o = 300 V
- Input inductors: $\mathbf{L_a} = \mathbf{L_b} = \mathbf{L_c}$ = 4 mH
- Output capacitors: $\mathbf{C_a} = \mathbf{C_b}$ = 600 μF
- Rated output power: **P** = 7.4 kW

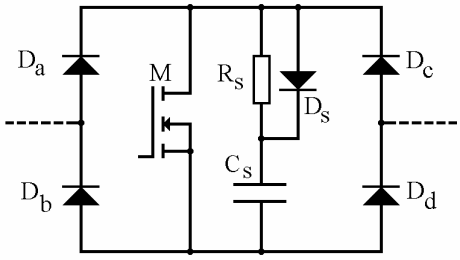

Fig. 8: Assembly for the bidirectional switches S_a, S_b and S_c.

Each of the bidirectional switches $\mathbf{S_a}$, $\mathbf{S_b}$ and $\mathbf{S_c}$ was assembled with a IRF740 MOSFET (**M**) connected between the DC nodes of a rectifier bridge, made with four SK3G/04 Semikron diodes ($\mathbf{D_a}$, $\mathbf{D_b}$, $\mathbf{D_c}$ and $\mathbf{D_d}$), as shown in Fig. 5. Other semiconductor switching devices, such as IGBTs or bipolar transistors could be used; high frequency performance is not a requisite, since the switching devices operate near line frequency.

Although the simulations showed that no overvoltages are present on the switches, the assembly can introduce a parasitic inductance. Therefore, it is convenient to have a small "snubber" circuit in parallel with each MOSFET. On the assembly shown in Fig. 5, $\mathbf{R_s}$ is a 1 kΩ × 5 W wire resistor, $\mathbf{C_s}$ is a 0.1 μF × 630 V polyester capacitor and $\mathbf{D_s}$ is a small 1N4004 diode.

$\mathbf{D_1}$ to $\mathbf{D_6}$ (Fig. 1b) are SKN12/12 Semikron rectifier diodes. The input inductors $\mathbf{L_a}$, $\mathbf{L_b}$ and $\mathbf{L_c}$ were constructed with ordinary silicon-steel *E-I* sheets, with air gaps to provide inductance adjustment. Each of the inductors weighed about 2.9 kg. A very simple open-loop control circuit was arranged in order to adjust simultaneously the conduction angle (α) of the three switches from zero to 30°.

Bench tests of the prototype were conducted with an assortment of high-power wire resistors connected as the load. The maximum output power delivered was 7.43 kW, with α adjusted to 30°. At that load condition, the measured output voltage was 291.5 V and the waveforms of the resulting input current and of the phase voltage are shown in Fig. 6. The Fourier Analysis of the input current issues a Total Harmonic Distortion (THD) of 6.56 % and the resulting power factor is 0.996. Although the laboratory AC source has three 20 μF capacitors on a "Y" connection to minimize intrinsic inductance, apparently they were not enough to ensure a pure sinusoidal AC source for high-power tests. In view of that limitation, the input AC voltage shown in Fig. 7 has an intrinsic distortion of about 3 % and the experimental THD is therefore higher than the theoretical value. For 7.43 kW output power, the measured *rms* input power was 7.66 kW, resulting in an efficiency of 97%.

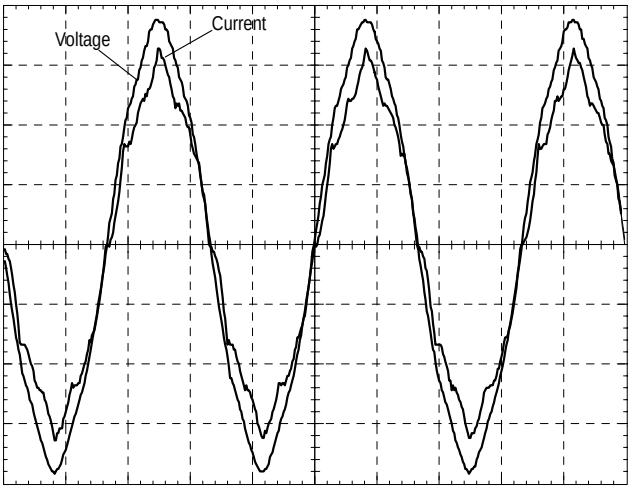

Fig. 6: Input Current and Voltage for 7.43 kW power output. Scales: Voltage = 50 V/div.; Current = 10 A/div.; Time = 5 ms/div.

In contrast to the topology proposed in [4], no overvoltage stresses are presented on the switches. Fig. 7 shows the drain-source voltage across the MOSFET and the external current on one of the bidirectional switches, for $\alpha = 30°$ and 7.43 kW power output condition. It can be seen that the MOSFET conducts current just for a short interval, so the *rms* value of that current is very low, and power loss is minimal.

Fig. 11 shows the output characteristic of the 7.4 kW prototype. It is evident that the conduction angle α can be used to control the output voltage over an extended power output range.

To verify the ability of the proposed rectifier to achieve a high power factor with constant output voltage, the DC output voltage of 291.5 V obtained at the 7.43 kW load condition was chosen as the goal value. On the following tests, for each load condition the conduction angle α was adjusted manually in order

to have 291.5 V for the output voltage.

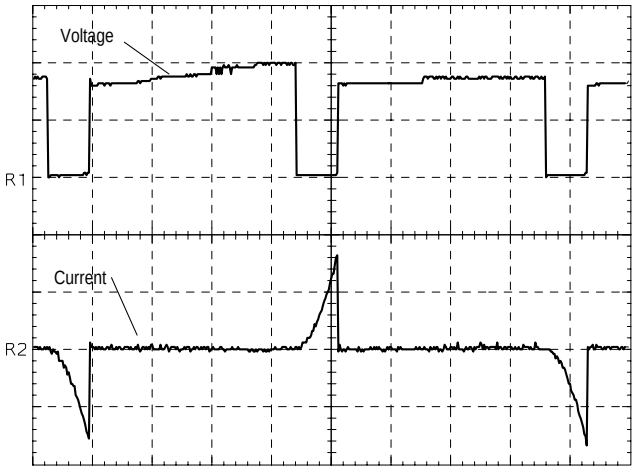

Fig. 7: Drain-Source Voltage on the MOSFET and external current of S_a, for $\alpha = 30°$.
Scales: Voltage = 100 V/div.; Current = 10 A/div.; Time = 2 ms/div.

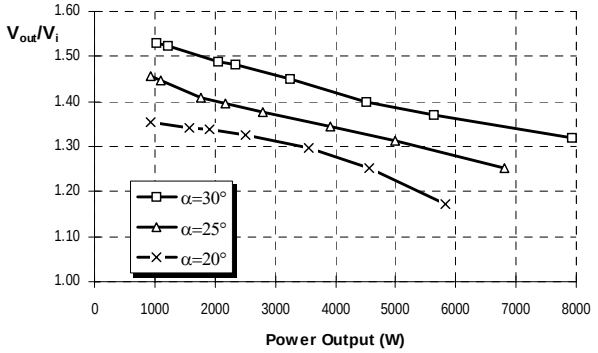

Fig. 8: Output characteristic of the 7.4 kW prototype.

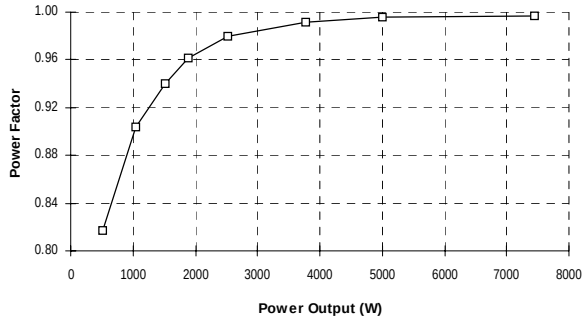

Fig. 9: Power Factor of the 7.4 kW prototype, measured at several load conditions and 291.5 V output voltage.

The results of the bench tests with constant output voltage are presented in Fig. 9 and Fig. 10. It is observed that the prototype can achieve a high power factor over an extended output power range, with regulated output voltage. Fig. 11 shows the variation of the conduction angle α, between 15° for 500 W output power and 30° for 7.43 kW output power.

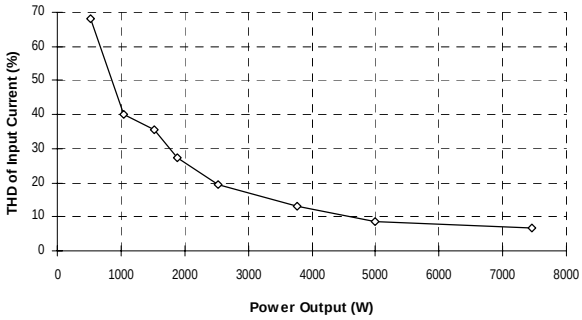

Fig. 10: Total Harmonic Distortion (THD) on the input current of the 7.4 kW prototype, measured at several load conditions and 291.5 V output voltage.

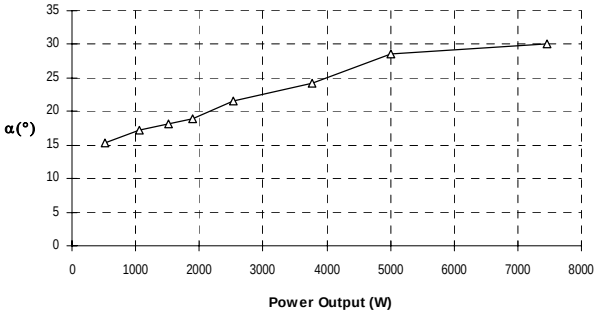

Fig. 11: Adjustments made on the conduction angle (α) of the switches S_a, S_b and S_c, on the 7.4 kW prototype, in order to obtain constant output voltage of 291.5 V.

After the promising results achieved with the 7.4 kW prototype, another converter was build, rated at 12 kW, with the same topology (Fig. 1b) and connected to the three-phase 220 V/127 V AC supply. The main components used in the second prototype were:

- Input Inductors: $\mathbf{L_a} = \mathbf{L_b} = \mathbf{L_c} = 1.9$ mH
- Output Capacitors: $\mathbf{C_a} = \mathbf{C_b} = 2250$ μF
- Diodes: $\mathbf{D_1} = \mathbf{D_2} = \mathbf{D_3}$ = Semikron SKN26/04
  $\mathbf{D_4} = \mathbf{D_5} = \mathbf{D_6}$ = Semikron SKR26/04
- MOSFETs for $\mathbf{S_a}$, $\mathbf{S_b}$ and $\mathbf{S_c}$: APT6040BN
- Diodes for $\mathbf{S_a}$, $\mathbf{S_b}$ and $\mathbf{S_c}$: Semikron SK3G10
- "Snubbers" for $\mathbf{S_a}$, $\mathbf{S_b}$ and $\mathbf{S_c}$: same as the 7.4 kW prototype.

For preliminary tests, the same gate pulse generator circuit used on the 7.4 kW prototype was used. The new prototype showed a similar behavior of the previously presented prototype. At 12.5 kW power output, with conduction angle $\alpha = 30°$, the main results were:

- Output voltage: 302.0 V
- Power Factor: 0.994
- THD of input current: 6.0 %

Although the prototypes showed a high power factor and low harmonic distortion of the input current for an extended range, it can be seen in Fig. 10 that the THD of the input current is quite high when the circuit operates at low-load condition. To achieve lower harmonic distortion at low-load situation, work is being performed in the direction of a different gate scheme for

low-level loads.

A closed-loop control circuit is also being build in order to perform constant-voltage output tests.

Conclusions

This paper presents a new AC to DC high power factor three-phase diode rectifier with three low-power and low-frequency four-quadrant switches. Two laboratory prototypes were evaluated through bench tests. The results showed that the proposed technique can be used to build new high power rectifiers and can be added to existing apparatus, since the main rectifier diodes are little affected by the presence of the bidirectional switches.

Although very similar to the topology presented in [4], the new converter shows some remarkable advantages:

- No connection is needed to the AC system neutral wire. As a result, the 3rd harmonic component was eliminated and the THD of the input current was reduced from 12% in [4] to 6 % (or less) in the new circuit.
- The power factor was increased and is almost unitary at the nominal load condition.
- The turn-off overvoltage presented on the circuit of [4] was also eliminated in the new topology.
- For the same values of the conduction angle α, the new converter showed a higher output voltage characteristic, what could be convenient for switch-mode power supply applications.

Other important features of the proposed rectifier are:

- A high power factor is achieved over an extended output power range.
- The rated power of each auxiliary switch is very low in contrast to the high output power of the rectifier. Therefore, the switches can be assembled with low cost semiconductor devices and power losses are minimal.
- As the auxiliary switches operate at low frequency, the gating circuit is elementary and there is no necessity of fast switching semiconductor devices.
- The turn-off voltage stresses across the semiconductor devices are low. No clamping circuits are necessary.
- The input inductors operate at low frequency, and were assembled using ordinary silicon-steel material for the cores. Although it is necessary to have inductance on the range of several mili-henry, the high magnetic flux density of the metal leads to small inductors. The cost of the low-frequency core material is also insignificant in contrast to the high-frequency ferrite material that would be necessary for building high-frequency inductors.
- The conduction angle of the switches can be adopted as the control variable to perform the output voltage regulation of the rectifier, while keeping the power factor near unity over a significant range of the output power.

Acknowledgment

E. L. M. Mehl would like to thank the Federal University of Paraná and the Brazilian Ministry of Education, under CAPES, for supporting his doctorate studies at the Federal University of Santa Catarina.

References

[1] PRASAD, A. R.; ZIOGAS, P. D.; MANIAS, S. An active power factor correction technique for three-phase diode rectifiers. In: IEEE POWER ELECTRONICS SPECIALISTS CONFERENCE, PESC'89. June 1989, p. 58-66.

[2] ISMAIL, E.; ERICKSON, R. W. A single transistor three-phase resonant switch for high quality rectification, In: IEEE POWER ELECTRONICS SPECIALISTS CONFERENCE, PESC'92. June-July 1992, p. 1341-51.

[3] ISMAIL, E.; ERICKSON, R. W. A new class of low cost three-phase high quality rectifiers with zero-voltage switching. In: IEEE APPLIED POWER ELECTRONICS CONFERENCE, APEC'93. March 1993, p. 182-9.

[4] FAGUNDES, J. C.; CRUZ, C. M. T.; BARBI, I. Active Power Factor Correction in a Three-Phase Rectifier by switching the AC Line Current. In: BRAZILIAN POWER ELECTRONICS CONFERENCE, 2. COBEP'93. Uberlândia, UFU/ SOBRAEP, 1993. p. 46-51.

[5] KOLAR, J. W.; ZACH, F. C. A novel three-phase three-switch three-level unity Power Factor PWM Rectifier, In: PCIM CONFERENCE, 28. Nürnberg, June 1994.